QUANTITATIVE DETERMINATION OF NUCLEAR PORE COMPLEXES IN CYCLING CELLS WITH DIFFERING DNA CONTENT

GERD G. MAUL and LARRY DEAVEN

From The Wistar Institute of Anatomy and Biology, Philadelphia, Pennsylvania 19104, and Los Alamos Scientific Laboratory, University of California, Los Alamos, New Mexico 87544

ABSTRACT

The number of pore complexes per nucleus was determined for a wide variety of cultured cells selected for their variable DNA content over a range of 1-5,600. The pore number was compared to DNA content, nuclear surface area, and nuclear volume. Values for pore frequency (pores/square micrometer) were relatively constant in the species studied. When the pore to DNA ratio was plotted against the DNA content, there was a remarkable correlation which decreased exponentially for the cells of vertebrate origin. Exceptions were the heteroploid mammalian cells which had the same ratio as the diploid mammalian cells despite higher DNA content.

The results are interpreted to mean that neither the nuclear surface, the nuclear volume, nor the DNA content alone determines the pore number of the nucleus, but rather an as yet undetermined combination of different factors. The surface and the volume of vertebrate nuclei do not decrease with decreasing DNA content below a given value. The following speculation is suggested to account for the anomalous size changes of the nucleus relative to DNA content in vertebrates. Species with small DNA complements have a relatively large proportion of active chromatin which determines the limits of the physical parameters of the nucleus. The amount of active chromatin may be the same for at least the vertebrates with low DNA content. At high DNA content, the nuclear parameters may be determined by the relatively high proportion of inactive condensed chromatin which increases the nuclear surface and volume.

The two membranes of the nuclear envelope are interrupted by nuclear pore complexes, the structure and possible function of which have been the subject of several reviews (9-13, 19, 20, 32, 35). These pore complexes could control the exchange of macromolecules between the two major compartments of the cell either by a change in total number of pores or by a selective filter mechanism. Feldherr (8) determined that gold particle size rather than pore frequency seemed to influence the exchange rate. Paine et al. (29) found that the pore complex has a patent radius of 45 Å and, therefore, allows free exchange of small molecules. No selective filter function other than pore size has been demonstrated up to now. An increase in the nuclear pore number, however, could be brought about experimentally in lymphocytes that had been stimulated with phytohemag-

glutinin (PHA) (23, 24), indicating a change in nuclear pore number during a change in metabolic activity. Also, the total pore number per nucleus doubled from a plateau in the G_1 phase to the end of the cell cycle in HeLa cells, and the pore-volume ratio stayed equal during this time (24). The question which arose from these observations is whether there is any relationship between the amount of DNA and the nuclear pore number and whether the volume or the surface of the nucleus are determining factors. Another possibility is that neither the DNA content, volume nor the surface of the nucleus determines the nuclear pore number. To compare cells of varying origins and DNA content, we had to analyze cells at the same activity. We selected proliferating cells in culture because they were engaged in a comparable activity, and because they had an added advantage in that their nuclear size could be determined with high accuracy in the live cells.[1]

MATERIALS AND METHODS

Some of the cell lines used in this investigation were obtained from the American Type Culture Collection (Rockville, Md.) (*Xenopus laevis,* kidney cells [A6]; mouse L cells [L929]; and African Green Monkey cells [CV1]). Others were obtained as follows: *Peromyscus crinitus* cells from Dr. T. C. Hsu (Anderson Hospital, Houston, Texas); *Rana pipiens* cells from Dr. J. J. Freed (Institute for Cancer Research, Philadelphia, Pa.); *Notophthalmus viridescens* cells from Dr. T. S. Reese (National Institutes of Health, Bethesda, Md.); *Drosophila* (S2) cells from Dr. I. Schneider (Walter Reed Hospital, Washington, D. C.); and yeast from Dr. L. Hartwell (University of Washington, Seattle, Wash.). The cell lines of the salamander *Triturus cristatus* (heart), and the toads *Xenopus laevis* (heart), and *Scaphiopus holbrooki* (heart) were established in our laboratory. WI38, HeLa, and CHO cells came from Wistar stocks. Chicken explants were made from 11-day-old embryos and used on the 7th day after explanting the tissue.

The cells were maintained in different media. *Triturus, Rana,* and *Xenopus* cells were established and maintained in Leibowitz medium, with 20% fetal calf serum diluted to 60% with H_2O at 24°C. *Scaphiopus* was established and maintained in MEM, with 20% fetal calf serum diluted to 80% with H_2O. Mouse L, HeLa, WI38, CV1, and CHO cells were maintained in MEM with 10% fetal calf serum. All media contained 0.1 mg/ml of streptomycin and 200 U/ml of penicillin, except the medium for *Scaphiopus,* in which fungal growth had to be suppressed initially by the use of Fungizone (E. R. Squibb & Sons, New York, N. Y.). *Drosophila* cells grew at 25°C in Schneider's medium with 10% heat-inactivated serum. Yeast (*Saccharomyces cerevisiae*) was grown according to Hartwell (17) at 24°C or with the same medium but containing 20% glycerol. After several days, the yeast adapted to this condition but grew very slowly.

Determinations of nuclear diameter by phase-contrast microscopy, of height by electron microscopy, and of pore frequency by freeze-etching were done on cells during the exponential growth phase (48 h after plating).

For determination of nuclear size the short and long axis of 50 live cells were measured and averaged separately. The average height was calculated from 20 electron micrographs of cross-sectioned cells embedded *in situ* (4). To estimate the surface area and the volume, we viewed the nucleus as a cylinder with an elliptical base, the rim of which then consisted of a semicircle (Fig. 1). The measured diameters were the sum of the major (or minor) axis of the ellipse, plus the radius of the rim (half the nucleus height). The average nuclear surface area, therefore, would equal the surface area of both bases of the cylinder, plus the product of the circumference of the cylinder's base and one-half the circumference of the circle, i.e., the circumference of the rim. Similarly, the volume of the nucleus was calculated from the cylinder's volume and the rim's volume. Therefore, the cylinder's volume equals the area of the base times the height of the cylinder. The rim's volume equals the area of the rim times the circumference of the cylinder's base.

HeLa, mouse L, and CHO cells were grown in suspension culture. Their nuclei appeared mostly round. The long and short axes of these nuclei were averaged, and the surface and volume were calculated as if the nuclei were spheres. The same calculations were performed for *Drosophila* cells, since these nuclei were round despite the fact that the cells grew on plastic or glass. The special conditions and calculations for the

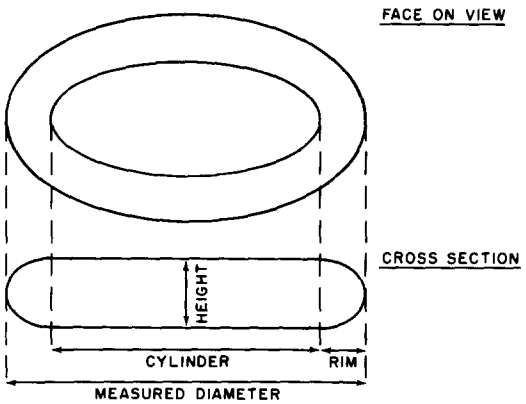

FIGURE 1 Schematic representation of the idealized nuclear shape for cells grown as monolayers. See text for rationale of surface and volume calculation.

[1] Maul, H. M. 1977. Comparison of nuclear surface and volume in cells grown in suspension vs. monolayers. Manuscript submitted for publication.

nuclear size in yeast will be given in the Results section, since these nuclei are so small that they cannot accurately be measured by light microscopy.

For freeze-etching, the cells were scraped from the tissue culture bottles with a rubber-tipped glass rod and resuspended in increasing concentrations of glycerol in medium up to 20% vol/vol within 10 min. After 30 min, the cells were gently concentrated in a tabletop centrifuge and frozen on gold specimen holders in liquid nitrogen-cooled Freon 22. The specimens were freeze-fractured in a Balzers' freeze-etch device (Balzers AG Balzers, Liechtenstein), etched for 1 min at 100°C and subsequently shadowed with platinum carbon (26). The replicas and sections were examined in an Hitachi HU11E microscope at 75 kV. For each set of negatives, a calibration was performed for the magnification (20,000) used to correct any instrumental variation. Pores were counted directly on the negatives with the aid of a stereoscope, and the areas were determined by planimetry. Care was taken to eliminate areas of the nuclear membrane with obvious curvature, to avoid an overestimate of pore frequency (Fig. 10).

For measurements of nuclear height, the cells were fixed *in situ* in 3-cm Falcon plastic petri dishes (Division of BioQuest, Oxnard, Calif.) with 3% glutaraldehyde in 0.1 M phosphate buffer with 1 mM $MgCl_2$ for 30 min, and postfixed in 1% OsO_4 in the same buffer for 30 min. The cells were then block-stained in 0.5% uranyl acetate in H_2O for 16 h at 60°C (22), rapidly dehydrated, and flat-embedded (4) in Epon 812. After removal of the plastic petri dish, the cells were reembedded so that they could be sectioned perpendicular to the plane of growth. This resulted in two lines of cells in each section. All nuclei seen in the microscope were photographed so long as they had not been tangentially sectioned. There was remarkably little variation in the height of most nuclei.

For autoradiography, cells were grown on small cover slips and incubated for 30 min with 4 μCi/ml of [H^3]thymidine (sp act 6.7, New England Nuclear, Boston, Mass.). After being coated with Kodak emulsion (NTB Type 2), exposed for 7 days, developed, and fixed, 500 cells were counted, and the number of labeled cells was determined.

Cells were sent to Los Alamos, New Mexico for DNA determination at the same passage level as that at which they were used for the analysis of nuclear pore number. DNA content per cell was determined by staining cell populations with acriflavine (6) and/or Mithromycin (5) and by analyzing them with the Los Alamos flow microfluorometer (FMF) (18). Fluorescence intensity was determined for the G_1 peak for each cell line and compared with that for the G_1 peak for Chinese hamster ovary (line CHO) cells. CHO cells contain 6.0×10^{-12} g of DNA as determined by Schmidt-Thannhauser analysis (21). In some instances, for cells with very low or very high DNA contents, direct comparison with CHO cells was not possible. In these cases, intermediate values between the cell lines were determined with the use of fluorescent microspheres or an electronic flasher component of the flow microfluorometer. Cells with very high DNA contents appear to be less amenable to flow microfluorometric analysis that mammalian cells, for as yet undetermined reasons. Therefore, in several cases, DNA determinations were made by the classical Feulgen technique. In all other cases, the flow system analysis has proven to be highly reproducible and accurate (±3-5%).

For cytophotometric determination of the DNA content, monolayers of cells were fixed and stained by a Feulgen procedure for DNA (7). Hydrolysis with 5 N hydrochloric acid at 24°C for 50 min was used to insure optimal dye binding. The cells were then incubated for 2 h in Schiff's reagent and rinsed in three changes of freshly prepared sulfide bleach, dehydrated, cleaned, and mounted in synthetic resin. The relative single-cell DNA content was determined with a Vickers M85 scanning microdensitometer (Vickers Instruments, York, England) as described by Goldstein (15, 16). Briefly, the specimen is viewed in a conventional microscope system, and an adjustable photo-electric grading system is used to define the measuring field. During operation, the measuring field is scanned by a flying spotlight probe. At the end of a scanning raster, the signals are electronically integrated. The contribution from the same measuring field without the nucleus is then obtained from a second scan in the immediate vicinity and subtracted from the first measurement. The values under the G_1 peak are averaged and used for the calculation of the DNA values.

RESULTS

The nuclear dimensions as seen with the phase microscope (Figs. 2-4) can be measured with great accuracy because the heterochromatin on the nuclear membrane increases its contrast. The error was less in the large nuclei of the *Notophthalmus* cells (Fig. 4) than in the smaller nuclei of the CV1 cells (Figs. 2 and 3) or in the nuclei of *Drosophila* cells that had a diameter of only about 5 μm (class interval, 1 μm). The elliptical shape of the nuclei was not always the ideal one shown in Fig. 2; the projection of some nuclei was more circular (Fig. 3), but there were no extreme deviations from the geometric shape. No measurements were made from giant nuclei in a population or from the small fraction of cells that were multinucleated. From Figs. 5 and 6, the basis for calculating the nuclear surface and volume can be observed. The cells were usually flat, and the nuclei are rounded at their margins. *Drosophila* cell nuclei are round despite the fact that they were grown on plastic (Fig. 7).

Determinations of errors in the different measurements revealed that no significant difference in the pore frequency existed between two replicas

from the same cell population frozen at the same time. As previously shown, there is a significant difference (9.6%; $P = 0.05$) within one replica if well frozen cells are compared to cells that contain ice crystals in their cytoplasm. These cells were judged to be dead since the same percentage of cells did not exclude dye (25). The reproducibility of the planimetry for the same set of areas was extremely good when the work was performed by the same person on the same type of paper on different days. A difference of up to 10% did occur when different persons performed the planimetry on the same set of areas, so the planimetry was subsequently performed by one person. After each set of micrographs, the electron microscope was calibrated to exclude instrument variability.

The determination of nuclear size was more problematic. 50 measurements of length and width proved sufficient to obtain reproducible results. If 50 measurements were repeated on the same slide, the length for *P. crinitus* cells was 15.92 ± 1.72 and 16.10 ± 1.27 ($P = 0.25$), respectively, and the width 9.92 ± 1.38 and 10.04 ± 1.03 ($P = 0.25$). The resultant size difference for surface and volume was about 2% in both cases. Some areas on the same slide were more confluent than others. Nuclei of confluent *P. crinitus* cells did not have a nuclear length and width different from those of cells at low density ($P = 0.2$; $P = 0.5$) if measured on the same slide. However, there was a significant difference when cells were plated and measured at different times. In CV1 cells, one measurement was 20.0 ± 2.18 μm vs. 20.4 ± 2.15 μm in length ($P = 0.2$) but 13.9 ± 1.99 μm vs. 11.3 ± 1.52 μm in width ($P = 0.001$). The resultant surface and volume differences were 12% and 15%, respectively. A significant difference in the width but not in the length of nuclei was found also if the cells were grown on glass rather than plastic. In *Notophthalmus viridescens* the *P*-value for nuclear length was 0.15 but for nuclear width was 0.05, resulting in about an 8% difference in surface and volume. For the spadefoot toad, the results were the same (length $P = 0.3$, width $P = 0.002$; 7% surface difference, 8% vol difference). The variability of the pores/μm^2 for different exponentially growing cultures of the same cell type has also been determined repeatedly. The difference was never more than 6% and usually between 2 and 3% (data are available on two series of comparably activated lymphocyte populations, 24).

Errors in the determination of nuclear height in flat cells have hardly any effect on determinations of nuclear surface, but they translate directly into errors in nuclear volume. In WI38 cells, a difference of 10% in height changes the nuclear surface by only 1.2% but changes the volume by 9.8%. The mean nuclear height as measured in the various experiments did not vary significantly (*N. viridescens* $P = 0.15$; CV1 cells $P = 0.35$).

Nuclear shape has little influence on the surface area and volume in flat cells. In "spherical" nuclei of cells grown in suspension culture there is a nuclear indentation at the cytocenter, which results in an overestimate of about 25% in volume and an underestimate of about 15% in surface.[1] The numbers in Table I represent the corrected values. Briefly, the indentation at the cytocenter results in a nuclear shape similar to the shape of an indented ball. Since most cells will appear round when the indentation is parallel to the optical axis, the volume will be extremely overestimated if the formula for a sphere is used. Measurements of nuclei seen with the indentation at right angles to the optical axis tend to underestimate the surface since one can imagine the indentation ballooned out. The indentation seems to be due to microtubules. If Colcemid was added to break the microtubules, the short diameter of the nucleus increased but not the long one. Our estimates also take into account folds of the nuclear membrane. The estimates of nuclear size were made on live cells in medium, but the pore frequency was determined on glycerinated cells. The effect of glycerol on nuclear size was therefore determined in chicken and WI38 cells. In WI38 cells, the nuclear length was 22.9 μm ± 2.2 and the width 11.8 ± 1.8 in the controls vs. 21.6 ± 2.3 and 11.7 ± 2.0 in the glycerinated cells. In a repeat of the measurements, the length differences were reversed, i.e., the control nuclei were slightly shorter. The differences are not significant. The same observation was made with chicken cells (23.3 ± 3.5 and 11.0 ± 2.0 μm vs. 23.1 ± 4.2 and 11.1 ± 2.1 μm). The standard deviation was always slightly larger in the glycerinated samples, probably because the fine line of the nuclear membrane was not so distinctly recognizable as in the controls, but the mean of the nuclear measurements did not show any significant difference. Methodological investigations on glycerin-treated cells have previously been reported for cells in suspension culture ("spherical cells") (24, 25).

From the determinations of error, the methodological error should be less than ±15%. Among the 10 determinations of nuclear pore number

TABLE I

Summary of Nuclear Parameters for Species with Different DNA Content

Species	Tissue	Culture Condition*	DNA Content	Surface	Vol.	Pores/ μm^2 ± SD	Pores/nucleus	Pores/ μm^3	Surface/DNA	Vol/DNA	Pores/DNA	Surface/Vol	Cells in S phase
			10^{-12} g	μm^2	μm^3				$\mu m^2/10^{-12}$ g	$\mu m^3/10^{-12}$ g	pores/10^{-12} g	$\mu m^2/\mu m^3$	%
Notophthalmus viridescens	lens	M	95.6‡	2,540	4,174	6.45 ± 1.4	16,383	3.9	26.7	43.7	171	0.61	20
Triturus cristatus	heart	M	59.6‡	1,672	1,748	7.61 ± 1.4	12,724	7.3	28.1	29.3	213	0.96	63
Rana pipiens	embryo	M	14.34§	625	627	7.90 ± 1.2	4,938	7.9	43.6	43.7	344	1.00	44
Xenopus laevis (A6)	kidney	M	7.68	340	294	10.05 ± 1.5	3,417	11.6	44.3	38.3	445	1.16	31
Xenopus laevis	heart	M	7.68	365	307	9.50 ± 2.1	3,468	11.3	47.5	40.0	452	1.19	38
Scaphiopus holbrooki	heart	M	3.78	271	197	9.45 ± 2.0	2,561	13.0	71.7	52.1	678	1.38	32
Peromyscus crinitus	lung	M	6.30	267	153	11.67 ± 1.8	3,116	20.4	42.4	24.3	495	1.75	39
Mouse L		S	13.80	467	435	10.83 ± 2.8	5,058	11.6	33.8	31.5	366	1.07	35
Human lymphocytes		S	6.24‖	254	232	8.41	2,136	9.2	40.7	37.2	342	1.09	–
Human WI38	lung	M	6.24	328	170	8.50 ± 1.3	2,788	16.4	52.7	27.2	447	1.93	44
Human HeLa	cervix	S	10.68	350	374	11.24 ± 1.8	3,934	10.5	32.8	35.0	368	0.94	41
African Green monkey (CVI)	kidney	M	13.96	498	421	8.59 ± 1.8	4,278	10.2	35.7	30.2	306	1.18	39
Chinese hamster (CHO)	ovary	S	6.00¶	221	188	9.44 ± 2.1	2,086	11.1	36.8	31.3	348	1.18	32
Chicken	embryo	M	2.68	308	210	9.29 ± 1.6	2,861	13.6	114.9	78.4	1,068	1.47	40
Tetrahymena pyriformis (GL)**		S	15.70‡‡	370	678	39 ± 9	14,430	21.3	23.6	43.2	919	0.55	–
Drosophila melanogaster (S2)	imaginal disc	M	0.30§§	90	78	12.62 ± 2.2	1,136	14.6	300.0	260.0	3,787	1.15	32
Saccharomyces cerevisiae		S	0.017‖‖	10.75	3.3	11.03 ± 3.1	119	35.8	632.4	195.3	7,000	3.24	–

* S = cells grown in suspension (spherical cells). M = cells grown in Falcon plastic flasks (monolayers; flat cells).

‡ The DNA data on *Notophthalamus viridescens* and *Triturus cristatus* were obtained cytophotometrically.

§ The value for *Rana pipiens* is an average of 10 FMF determinations.

‖ The value for human lymphocyte was set equal to that of the human WI38 cells.

¶ The FMF value for CHO cells was used as a standard for comparing all other data. CHO cells were assumed to have 6.0×10^{-12} g of DNA as determined by Kraemer et al. (21).

** Data from Wunderlich (36).

‡‡ DNA value for *Tetrahymena* was obtained from Scherbaum et al. (30).

§§ The *Drosophila* DNA values are about 25% higher than the diploid DNA content of 0.24×10^{-12} g (2).

‖‖ *S. cerevisiae* DNA content from Bicknell and Douglas (1).

which had been repeated, none showed a difference of 20% except those for yeast, but in this instance the growth conditions were different. Variability with different growth conditions has not been determined yet.

The DNA content of *Triturus* and *Notophthalmus* can be determined cytophotometrically. As controls, chicken explants, WI38, and CV1 cells were also measured cytophotometrically. The ratios determined between the DNA values of the G_1 peaks obtained by flow microfluorometry and the mean of arbitrary units of the G_1 peaks varied between 2.71 and 2.73 (arbitrary $U/10^{-12}$ g) for the cell types stained in the same dish and measured on the same day (see Fig. 11 *a* and *b* for overlap of FMF and cytophotometrically obtained data). In both types of measurements, one finds the G_2 peaks slightly larger than twice the G_1 peak. The average ratio was used to calculate the DNA value for the G_1 peak of *Triturus* and *Notophthalmus* cells. For *S. cerevisiae,* data from Bicknell and Douglas (1) were used.

Because of the small size of the yeast nucleus and the cells' high densities, no direct measurements could be made on live cells with the contrast microscope. Also, because of the great curvature of the nuclear membrane fracture faces, measurements for the surfaces had to be corrected. The nuclear size had to be estimated from cross fractures. In Fig. 8, a face-on view of the yeast nuclear envelope is shown, and in Fig. 9 a cross fracture. Both figures represent the fractures obtained and indicate that the nucleus is primarily a sphere in the preparation analyzed (see, however, reference 31). The nuclear membrane areas as well as the cross fractures at right angles were measured in 0.05 μm class intervals. From the the distribution in Fig. 12, the maximum diameter of the membrane fracture faces can be observed not to overlap significantly the diameters of the cross fractures of the nuclei. This feature indicates that at a given fracture angle (about 127°) the membrane splits, whereas if the angle is more acute (<127°) the membrane is cross fractured, i.e., at a fracture angle of exactly 90° on a sphere, the maximum diameter would result.

For the nuclear diameter the mean was not used, as this would have resulted in an underestimate; rather, we used the value for the shoulder at the large diameters (1.85 μm). The precipitous drop indicates that few nuclei are larger, and therefore represents the maximal diameter. There seems to be only a narrow range of nuclear diameters. If 1.85 μm is used as the diameter, the surface of the average yeast nucleus is 10.75 μm^2 and the vol 3.32 μm^3. Calculation of surface of a segment from its projection (the average of the measured diameters of the nuclear surfaces) results in a correction factor of 0.882. The value of 12.51 pores/μm^2 determined from the micrograph is, therefore, only 11.03 pores/μm^2. The resulting average pore number per nucleus (119 pores) is substantially lower than the one calculated by Moor and Mühlethaler (26) for old or stationary yeast cells.

In another experiment, yeast cells were kept in medium containing 20% glycerol. They grew much slower and had a smaller corrected pore frequency (8.92 μm^2), a smaller surface (9.08 μm^2), a smaller volume (2.5 μm^3) and, therefore, a smaller pore number (81 pores per nucleus), i.e., there were 32% fewer nuclear pores in the slow growing yeast.

For convenience in determining nuclear size, mammalian cells with spherical nuclei had initially been selected. Also, the DNA content of CHO, HeLa, and mouse L cells had already been determined repeatedly (L. L. Deaven, unpublished observations). The pore number of cycling human lymphocytes had been estimated previously (24). As can be seen from Fig. 16, the pore/DNA ratio was approximately the same in these four cell lines despite a more than twofold variation in DNA content. We decided to extend the number of different cell lines and select them according to different DNA content. Table I provides the summary of the data collected during this extended investigation, and reveals an obvious increase in nuclear surface with increasing DNA content; this increase is not proportional, however. For the cells of vertebrate origin, there is little increase in nuclear surface from 2.6 pg to 7.7 pg DNA, followed by a more or less linear increase to 95 pg DNA. The nuclei of *R. pipiens* cells are an exception, in that they have a relatively large surface (Fig. 13).

Another unexpected finding is the lack of increase in nuclear volume with increasing DNA content in the flat nuclei of normal diploid chicken cells, spadefoot toad cells, WI38 cells, and *P. crinitus* cells (Fig. 14). The nuclear volume in the heteroploid cells increases with the DNA content so that the nuclear volume/DNA ratio remains about the same. If we compare the nuclear volume/DNA ratio to the total DNA content of all vertebrate cells investigated, no strict correlation

seems to exist (Fig. 15). A line was drawn through the values of those diploid cells with normal DNA content in which no increase in nuclear volume was observed. Generally speaking, a clustering could be observed around a nuclear volume-to-DNA ratio of 30 $\mu m^3/10^{-12}$ g.

If the nuclear pore/DNA ratio vs. the DNA content is plotted, a rather unexpected relationship becomes apparent (Fig. 16). The pore/DNA ratio decreases most rapidly in nuclei with a low DNA content. In nuclei with a higher DNA content, the pore-to-DNA ratio may level off asymptotically due to the continuing decrease in nuclear surface/DNA ratio, but also due to a drop in the pore frequency in nuclei with an extremely large DNA content. The very high pore/DNA ratios of *Drosophila* (3787) and yeast cells (6611) have not been included in Fig. 16 since their DNA value is so low that no accurate representation can be given in the graphic display. There is, however, no asymptotic increase seen if a log scale is used for plotting the data.

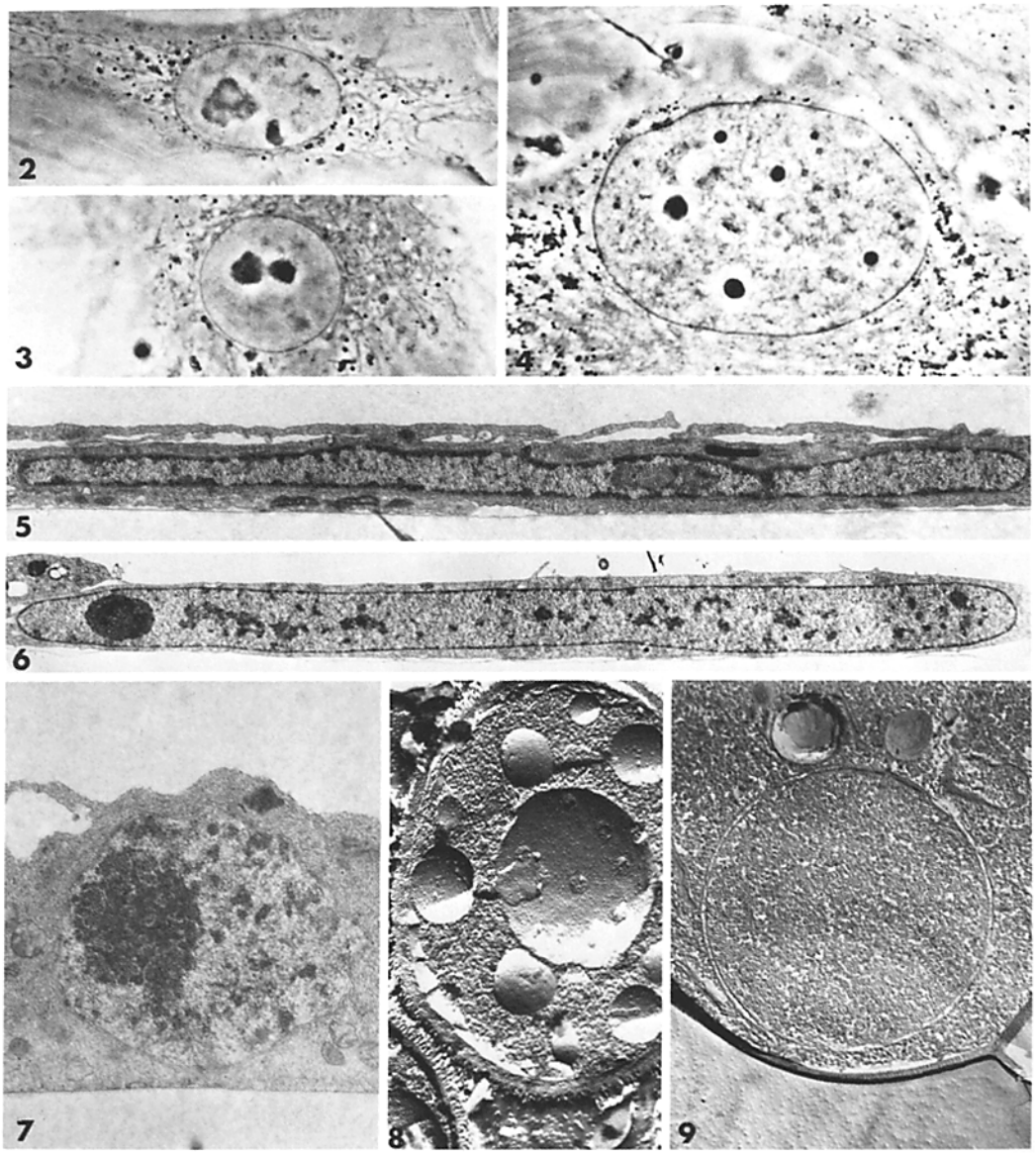

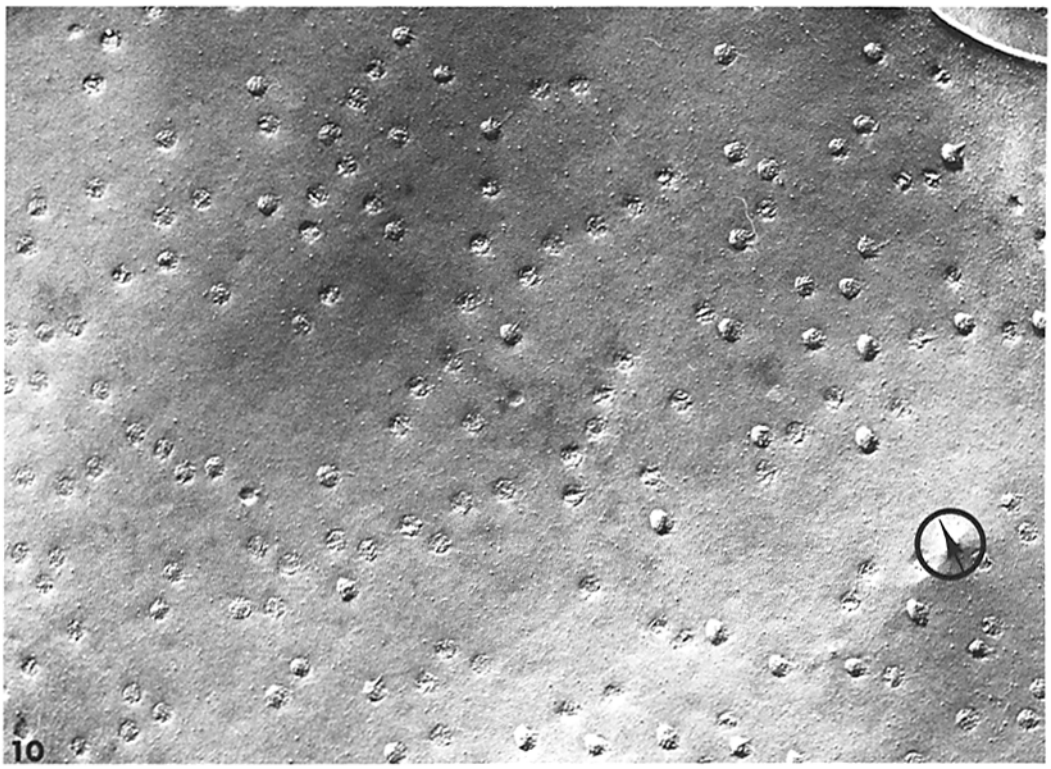

FIGURE 10. Nuclear surface of *Triturus cristatus* exposed by freeze-etching for the determination of pores/unit area. × 30,000. Arrow indicates direction of shadow.

FIGURE 2 Phase-contrast micrograph of a nucleus from a CV1 cell in culture, demonstrating the predominant elliptical shape. × 1,000.

FIGURE 3 Phase-contrast micrograph of a nucleus of a CV1 cell in culture, demonstrating the more circular shape. × 1,000.

FIGURE 4 Phase-contrast micrograph of an *N. viridescens* nucleus. × 1,000.

FIGURE 5 Cross section of a WI38 cell for the determination of nuclear height. The nuclei are very flat and without major folds. × 10,000.

FIGURE 6 Cross section through an *N. viridescens* nucleus, showing heterochromatin in the middle of the nucleus. × 4,000.

FIGURE 7 Cross section of a *Drosophila* cell nucleus for nuclear height determination. The nuclei were round despite monolayer culture. × 10,000.

FIGURE 8 Face-on view of the nuclear membrane of *S. cerevisiae*. Most exposed nuclear membrane fractures showed a great curvature. Therefore, the determination of the projected area would be an overestimated pore frequency. × 20,000.

FIGURE 9 Cross-fracture of the nucleus of *S. cerevisiae*. The outline was mostly round, indicating a spherical nucleus. × 20,000.

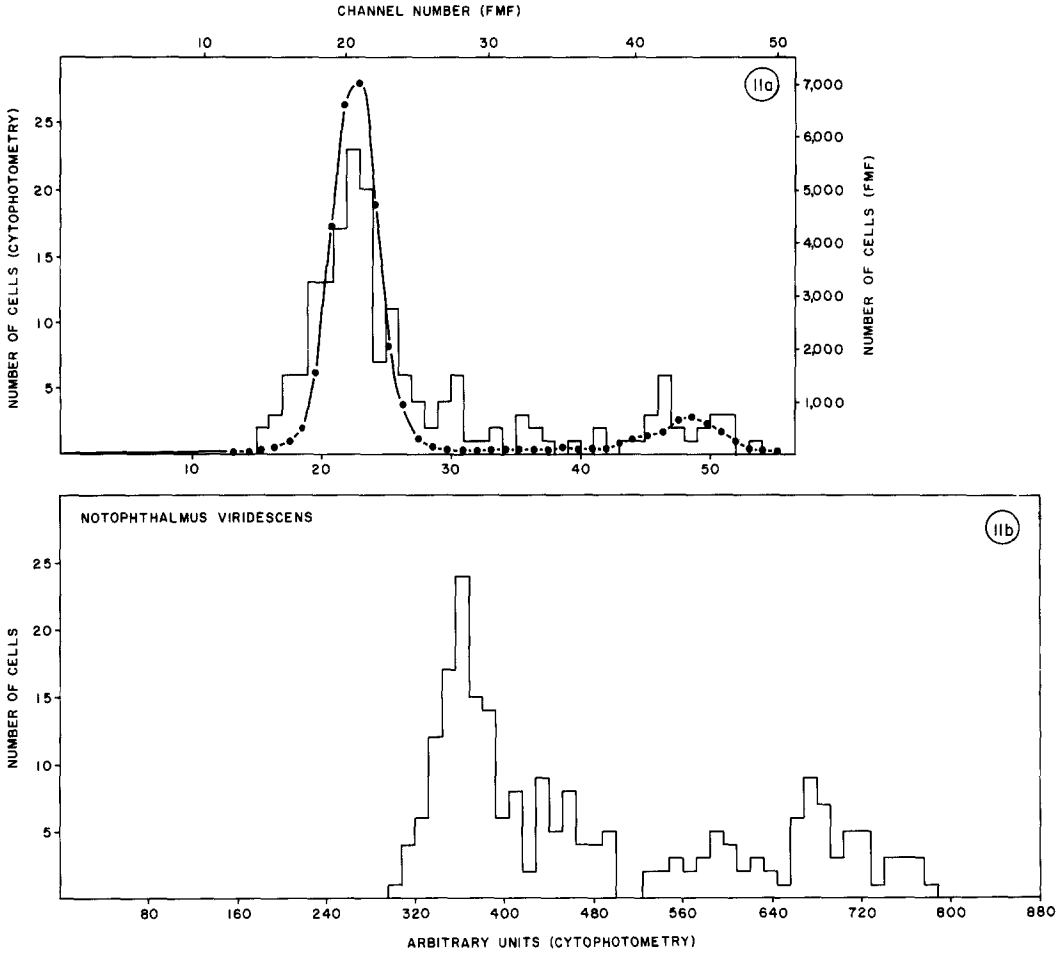

FIGURE 11 (*a*) Superimposition of DNA measurements obtained by flow microfluorimetry (●—●) and cytophotometry of WI38 cells in arbitrary units (block diagram). (*b*) Cytophotometrically obtained data for *N. viridescens* in arbitrary units. The value for the G_1 peak for *T. cristatus* and *N. viridescens* was determined from these data.

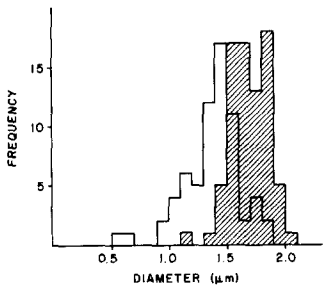

FIGURE 12 The diameter of exposed yeast nuclear surfaces (open area) and the diameter of cross-fractured yeast nuclei (hatched area) do not overlap much.

Most nuclear surface-to-volume ratios ($\mu m^2/\mu m^3$) are about 1.2. The lowest ratio (0.61) is that of *N. viridescens* with the highest DNA content; the highest ratio (3.24) is that of yeast with the lowest DNA content. Among the vertebrates, the higher ratio is found for the lung cells of man and mouse. The basic tendency of pore/volume ratio is that it is rather equal over a wide range of DNA values. There is an abrupt drop in the amphibian nuclei with high DNA content but not in the toad with low DNA content. Also, there is a relatively high ratio for both normal lung cell lines.

The proportion of thymidine-labeled cells after a 30-min pulse was used to determine whether or not a cell population was cycling. The lowest number of labeled cells was found in the extremely slow growing *N. viridescens* cells, which have an approx. 90 h doubling time (T. S. Reese, personal communication). This is in strong contrast to our *T. cristatus* cell line which, at its 34th passage,

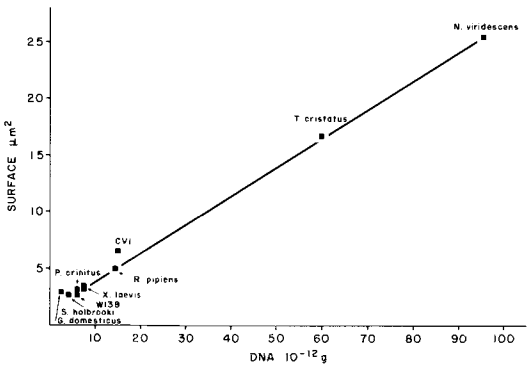

FIGURE 13 The nuclear surface does not increase linearly over the DNA range in vertebrates. It barely changes over a more than twofold DNA increase in the lower DNA range, but seems to increase linearly in the upper DNA ranges.

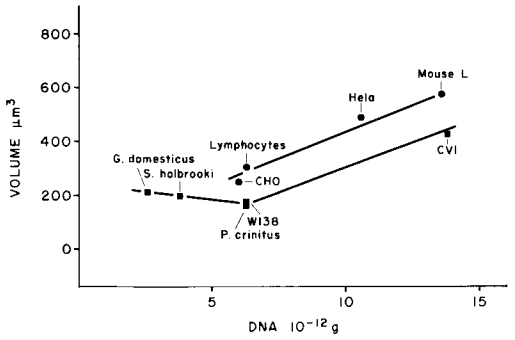

FIGURE 14 The nuclear volume drops slightly over a more than twofold increase in DNA content of flat (■) diploid cells in culture. The volume for spherical (●) nuclei of mammalian origin becomes larger with an increase in DNA content due to heteroploidy. The apparently larger volume of diploid spherical nuclei relative to the flat nuclei is due to a systematic error in volume determination. Table I gives the corrected values.

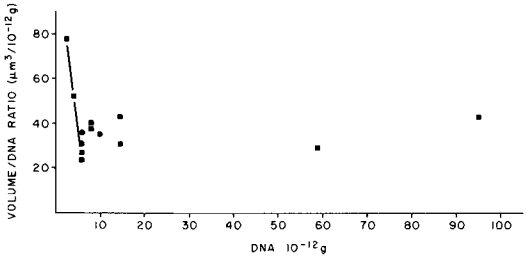

FIGURE 15 The volume to DNA ratio ($\mu m^3/10^{-12}$ g) scatters around 30. The line connects the values for flat (■) nuclei of the diploid cells of chicken, spade foot toad, WI38, and *P. crinitus*. The values for spherical (●) nuclei were corrected for the error in volume determination.

grows rather rapidly with a doubling time of less than 48 h (63% cells in S phase).

DISCUSSION

Nuclear pore complexes are localized on the interface between the two major cellular compartments, the cytoplasm and the nucleoplasm. The functions of this structure in the nuclear membrane *a priori* relate to nuclear-cytoplasmic exchange, and a large number of publications have dealt with these questions (for review, see references 9–13, 19, 20, 32, and 35).

In HeLa cells during the cell cycle, the number of pore complexes doubles from a G_1-phase plateau to the end of the cell cycle. During this time the ratio of pores-to-unit volume stayed the same (about 6.2 pores/μm^3) (24). Also, human lymphocytes, when transformed to blasts by PHA, and when cycling, had a similar number of pores/μm^3 (5.8 vs. 6.2) and about the same number of pores if one corrected for the differing DNA content. We, therefore, asked whether the DNA content or the nuclear volume determined the pore number in proliferating cells.

The pore/DNA ratio was found to be equal for human lymphocytes, CHO, HeLa, and mouse L cells over a wide range of DNA content. For those cells with flat nuclei, a quite different pattern of the pore/DNA ratio became evident. Basically, it was lower in nuclei with higher DNA values. The large pore/DNA ratio in the lower range of DNA values is related to the fact that nuclear size, i.e., surface and volume, did not decrease with decreasing DNA values below those for mammalian cells. The reason for this is not clear. However, one could speculate that for all vertebrate cells about the same amount of chromatin must be active for proliferative processes, that this DNA largely determines the size of the nucleus, and, also, that the condensed chromatin occupies little space relative to its amount of DNA. In cells with exceptionally large amounts of inactive DNA relative to the active DNA, the size of the nucleus will depend on this inactive DNA. Such a speculation would also explain the equal pore/DNA ratio in normal and heteroploid mammalian cells despite increasing DNA content by assuming that, upon addition of chromosomes, proportionately more membrane-bound and active chromatin is present. Not all the evolutionary increase in DNA may be active DNA (volume increase) or membrane-bound DNA (surface increase) but may consist of satellite DNA, of other genes added by tandem gene duplication that are not used in normal cell

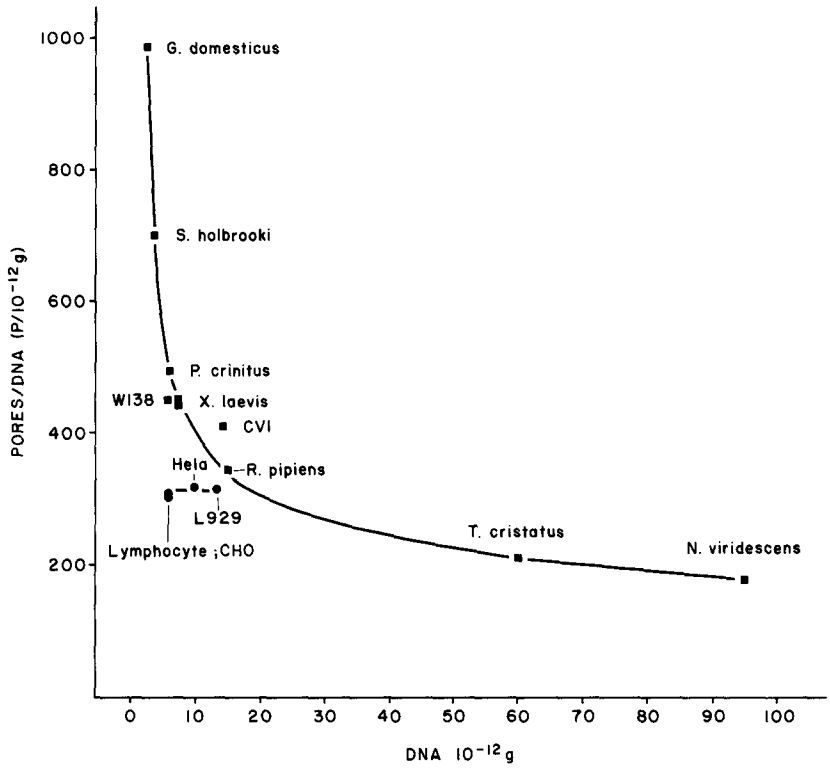

FIGURE 16 The pore to DNA ratio is plotted vs. the DNA content of all vertebrate cells investigated. All flat nuclei can be connected by a line indicating an asymptotic decay. The pore to DNA ratio for the spherical (●) mammalian nuclei in contrast are the same over a range of DNA content from 6.0 to 13.8 × 10^{-12} g. Uncorrected values were used to separate the two lines.

functions during proliferation, or of secondary silencing after polyploidization steps (28). The inactive or condensed chromatin will then add little volume relative to its amount of DNA.

Since there is an obvious relationship between the surface area and the DNA content, we may have to look for an explanation that involves this parameter. The number of pores per nucleus in proliferating cells is strongly determined by the surface area and only somewhat modified by the pore frequency. The rather similar pore frequency in eucaryotes with the lowest DNA content and in those with DNA contents 500 times higher is surprising and shows that pore frequency data alone are useless. The data may indicate, though, that the pore frequency is determined by some as yet unknown chromatin membrane property. The same range of pore frequencies has been reported for plants by Branton and Moor (3), Severs and Jordan (31), and Thair and Wardrop (34). They are well below the maximal pore frequency of about 68 pores/μm^2 (23). The basic data on *Tetrahymena* (36) have been included in our Table I since this proliferating ciliate with its macronucleus is an exception to the haploid or diploid cells investigated by us, in that it has a very high pore frequency and contains many times its diploid genome. The surface/DNA ratio, volume/DNA ratio, as well as the pore/DNA ratio, are within the range of those of the diploid cells. Other cell types with very high pore frequencies in the nuclear membrane are specialized, such as oocytes with the germinal vesicle with highly reiterated ribosomal DNA, the polytene salivary gland cells (13, 27), the malpighian cells (33), and the alga *Acetabularia* with the polyploid macronucleus (14, 38). Cells with high pore frequencies tend to be polyploid and nondividing.

From our results, we conclude that neither the surface, the volume, nor the DNA content alone determines the total pore number. We may have to assume a combination of several parameters, depending on the amount of active DNA. The narrow range of pore frequencies and the initially

nonlinear relationship of surface with DNA content also suggest an influence that is exerted by membrane-bound DNA. This DNA may occupy the same surface in birds, frogs, and mammals as long as its amount is not greater than that of mammals. The approximately equal surface DNA ratio for "spherical" and flat mammalian nuclei (if spherical nuclei are corrected for shape-related underestimate of surface and overestimate of volume) strengthens this assumption.

The basic concept that the total nuclear pore number depends on the activity of the cell has been shown for PHA-activated lymphocytes (23, 24). The increase in pore frequency in activated lymphocytes has been corroborated by Wunderlich et al. (37), using concanavalin A as a mitogen. The same cell type, thus, can have widely different numbers of nuclear pores, depending on its metabolic state. Our comparison of varying cell lines is only valid if one assumes approximately equal activity during proliferation. This may be the case for the cells of vertebrate origin but certainly not for yeast, *Drosophila*, and *Tetrahymena*.

We would like to thank all the individuals from whom we have obtained cell lines. The expert technical assistance of Mrs. Patricia Connelly, Mr. Joseph Weibel, and Mr. Howard Nathan is highly appreciated. We also thank Dr. Gary Grove for instructions on the Vickers M85 scanning microdensitometer, and Dr. H. G. Callan for supplying us with two specimens of *Triturus cristatus* from his backyard in Scotland.

This investigation was supported by U. S. Public Health Service research grants GM21615 from the National Institute of General Medical Sciences and CA10815 from the National Cancer Institute, and, in part, under the auspices of the U. S. Energy Research and Development Administration. G. G. Maul is a recipient of a Faculty Research Award (FRA 118) from the American Cancer Society.

Received for publication 11 August 1976, and in revised form 20 December 1976.

REFERENCES

1. BICKNELL, J. N., and H. C. DOUGLAS. 1970. Nucleic acid homologies among species of *Saccharomyces*. *J. Bacteriol.* **101**:505–512.
2. BONNER, J., and J.-R. WU. 1973. A proposal for the structure of the *Drosophila* genome. *Proc. Natl. Acad. Sci.* **70**:535–537.
3. BRANTON, D., and H. MOOR. 1964. Fine structure in freeze-etched *Allium cepa* root tips. *J. Ultrastruct. Res.* **11**:401–411.
4. BRINKLEY, B. R., P. MURPHY, and L. C. RICHARDSON. 1967. Procedure for embedding *in situ* selected cell cultures *in vitro*. *J. Cell Biol.* **35**:279–283.
5. CRISSMAN, H. A., and R. A. TOBEY. 1974. Cell-cycle analysis in 20 minutes. *Science (Wash. D. C.).* **184**:1297–1298.
6. DEAVEN, L. L., and D. F. PETERSEN. 1974. Measurements of mammalian cellular DNA and its localization in chromosomes. *Methods Cell Biol.* **8**:179–204.
7. DECROSSE, J. J., and N. AIELLO. 1966. Feulgen hydrolysis: effect of acid and temperature. *J. Histochem. Cytochem.* **14**:601–604.
8. FELDHERR, C. M. 1969. A comparative study of nucleocytoplasmic interactions. *J. Cell Biol.* **42**:841–845.
9. FELDHERR, C. M. 1972. Structure and function of the nuclear envelope. *Adv. Cell Mol. Biol.* **2**:273–307.
10. FRANKE, W. W. 1970. On the universality of the nuclear pore complex structure. *Z. Zellforsch Mikrosk Anat.* **105**:405–429.
11. FRANKE, W. W. 1974. Structure, biochemistry and functions of the nuclear envelope. *Int. Rev. Cytology (Suppl.)* **4**:72–236.
12. FRANKE, W. W. 1974. Structure and biochemistry of the nuclear envelope. *Philos. Trans. R. Soc. Lond. Biol. Sci.* **268**:67–93.
13. FRANKE W. W., and U. SCHEER. 1974. Structures and functions of the nuclear envelope. *In* The Cell Nucleus. H. Busch, editor. Academic Press, Inc., New York, **1**:219–347.
14. FRANKE, W. W., H. SPRING, U. SCHEER, and H. ZERBAN. 1975. Growth of the nuclear envelope in the vegetative phase of the green alga *Acetabularia*. Evidence for assembly from membrane components synthesized in the cytoplasm. *J. Cell Biol.* **66**:681–689.
15. GOLDSTEIN, D. J. 1970. Aspects of scanning microdensitometry. I. Stray light (glare). *J. Microsc. (Oxf.).* **92**:1–16.
16. GOLDSTEIN, D. J. 1971. Aspects of scanning microdensitometry. II. Spot size, focus, and resolution. *J. Microsc. (Oxf.).* **93**:15–42.
17. HARTWELL, L. H. 1970. Periodic density fluctuation during the yeast cell cycle and the selection of synchronous cultures. *J. Bacteriol.* **104(3)**:1280–1285.
18. HOLM, D. M., and L. S. CRAM. 1973. An improved flow microfluorometer for rapid measurement of cell fluorescence. *Exp. Cell Res.* **80**:105–110.
19. KAY, R. R., and I. R. JOHNSTON. 1973. The nuclear envelope. Current problems of structure and function. *Sub-Cell. Biochem.* **2**:127–166.
20. KESSEL, R. G. 1973. Structure and function of the nuclear envelope and related cytomembranes. *Prog. Surf. Membr. Sci.* **6**:243–329.
21. KRAEMER, P. M., D. F. PETERSEN, and M. A. VAN DILLA. 1971. DNA constancy in heteroploidy and

the stem line theory of tumors. *Science* (*Wash. D. C.*). **174:**714–717.

22. LOCKE, M., N. KRISHMAN, and J. T. MCMAHON. 1971. A routine method for obtaining high contrast without staining sections. *J. Cell Biol.* **50:**540–544.
23. MAUL, G., J. W. PRICE, and M. W. LIEBERMAN. 1971. Formation and distribution of nuclear pore complexes in interphase. *J. Cell Biol.* **51:**405–418.
24. MAUL, G. G., H. M. MAUL, J. E. SCOGNA, M. W. LIEBERMAN, G. S. STEIN, B.Y-L HSU, and T. W. BORUN. 1972. Time sequence of nuclear pore formation in phytohemagglutinin-stimulated lymphocytes and in HeLa cells during the cell cycle. *J. Cell Biol.* **55:**433–447.
25. MAUL, H. M., G. G. MAUL, and A. WESSING. 1972. Artifacts occurring during freeze-etch preparation. Proceedings of the 13th Annual EMSA Meeting. 296–297.
26. MOOR, H., and K. MÜHLETHALER. 1963. Fine structure in frozen-etched yeast cells. *J. Cell Biol.* **17:**609–628.
27. MOOR, H. 1967. As quoted by B. J. Stevens and J. André. The nuclear envelope. *In* Handbook of Molecular Cytology. Lima de Faria, editor. North Holland Publishing Company, Amsterdam. 837–871.
28. OHNO, S. 1970. Evolution by Gene Duplication. Springer-Verlag New York Inc., New York.
29. PAINE, P. L., L. C. MOORE, and S. B. HOROWITZ. 1975. Nuclear envelope permeability. *Nature* (*Lond.*). **254:**109–114.
30. SCHERBAUM, O. H., A. L. LOUDERBACK, and T. L. JAHN. 1959. DNA synthesis, phosphate content and growth in mass and volume in synchronously dividing cells. *Exp. Cell Res.* **18:**150–166.
31. SEVERS, N. J., and E. G. JORDAN. 1975. Nuclear envelope changes related to cell activation in *Helianthus tuberosus* L. *Experientia* (*Basel*). **31(11):**1276–1278.
32. STEVENS, B. J., and J. ANDRÉ. 1969. The nuclear envelope. Handbook of Molecular Cytology. L. Faria, editor. North-Holland Publishing Company, Amsterdam. 837–871.
33. TEIGLER, D. J., and R. J. BAERWALD. 1972. A freeze-etch study of clustered nuclear pores. *Tissue Cell.* **4:**447–456.
34. THAIR, B. W., and A. B. WARDROP. 1971. The structure and arrangement of nuclear pores in plant cells. *Planta* (*Berl.*) **100:**1–17.
35. WISCHNITZER, S. 1973. The submicroscopic morphology of the interphase nucleus. *Inter. Rev. Cytol.* **34:**1–48.
36. WUNDERLICH, F. 1972. Macronuclear envelope of *Tetrahymena pyriformis* GL in different physiological states. V. Nuclear pore complexes—a controlling system in protein-biosynthesis? *J. Membr. Biol.* **7:**220–230.
37. WUNDERLICH, F., D. F. H. WALLACH, W. SPETH, and H. FISCHER. 1974. Differential effects of temperature on the nuclear and plasma membranes of lymphoid cells. *Biochim. Biophys. Acta.* **373:**34–43.
38. ZERBAN, H., and G. WERZ. 1975. Changes in frequency and total number of nuclear pores in life cycle of *Acetabularia*. *Exp. Cell Res.* **93(2):**472–477.